

The importance of instrument location on barometric pressure-induced noise

Holger Steffen*

Institute of Geological Sciences, FU Berlin
Malteserstr. 74-100, Haus D
D-12249 Berlin / Germany

Abstract

Barometric pressure-induced noise in records of broadband seismometers, strainmeters and tiltmeters is one of the major limiting factors in analyzing the data for studies of the Earth's interior structure and properties. Even the instruments at the Black Forest Observatory (BFO), installed in a depth of 170 m in a mountain behind an air-lock door, are influenced. We investigate the physical transfer mechanisms for pressure-induced noise with the help of a Finite Element model of the BFO, emphasizing the effect of pressure changes on the horizontal components at different locations inside a vault, e. g. on piers and in niches. The results show noise amplification factors of up to 37 within a distance of 1 m, and changes in the direction of the measured components. Each component is influenced differently, which makes it difficult to determine the best location to place. In addition, former results can be confirmed and suggestions for a correction can be drawn.

1 Introduction

The data of seismometers, strainmeters, and tiltmeters have been successfully used for studies of the Earth's interior. Unfortunately, extracting more detailed information is limited due to barometric pressure-induced noise, which is superimposed on the signals of interest, e. g. longperiod seismometer and strainmeter records (e. g. Sorrels, 1971; Sorrels et al., 1971; Beauvuin et al., 1996; Zürn, 2002; Kroner et al., 2005; Zürn & Wielandt, 2006). The removal or likewise reduction of the disturbing signals is difficult, because the physical transfer mechanisms for pressure-induced noise especially in horizontal components are not well understood. Hence, in the last years many studies have been dedicated to barometric pressure-induced noise and its removal in

*E-Mail: hsteffen@zedat.fu-berlin.de

records of longperiod horizontal components (e. g. Fischer, 2002; Zürn, 2002; Zürn & Neumann, 2002; Kroner et al., 2005; Lambotte et al., 2006; Steffen et al., 2006; Zürn et al., 2006).

The Black Forest Observatory Schiltach (BFO; 48.33° N, 8.33° E; see Emter et al., 1999, for more information), located in a former mine, is characterised by a low noise level (Beauduin et al., 1996; Freybourger et al., 1997). Still, the instruments in 170 m depth behind an air-lock door (Fig.1) are affected by barometric-pressure changes, which implies the existence of transfer mechanisms related to the local setting. These mechanisms can be studied using the Finite Element (FE) approach. Thus, a FE model of the BFO is developed, including the main topographic structures and the gallery, and allowing the investigation of different loading scenarios. A detailed description of the first results can be found in Steffen et al. (2006). These results do not include the effects on different locations inside a vault, which will be the aim of this paper.

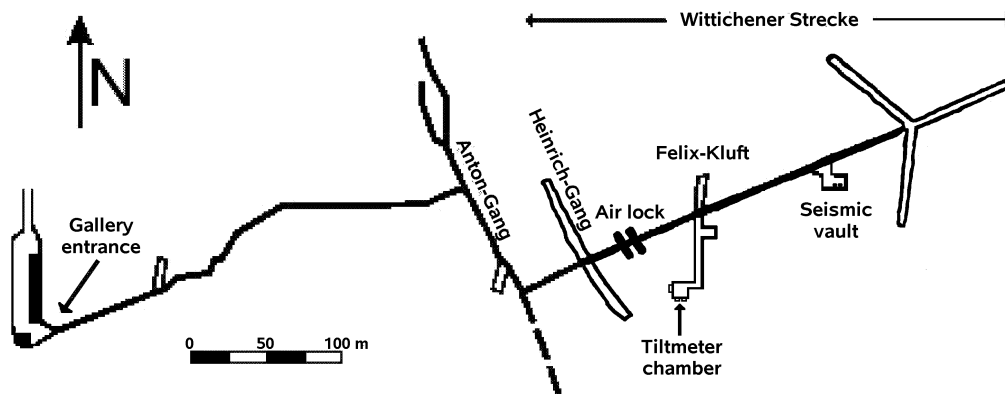


Figure 1: Sketch of the BFO. The “Felix-Kluft” with the tiltmeter chamber and the seismic vault with the long–period STS–1 seismometer can be found along the Wittichener Strecke behind the air lock.

2 Finite Element Modelling

The BFO model with its dimension is shown in Figure 2a. It is based on the model “litho” from Steffen et al. (2006) and includes new features: the “Felix-Kluft” with the tiltmeter chamber and piers in the seismic vault (Figs. 1 and 2b). The “Felix-Kluft”, a smaller cavity than the “Heinrich-Gang”, is located around 90 m west of the seismic vault. At its southwestern end the tiltmeter chamber can be found. Here, three niches are modelled, two in the southern and one in the western wall (Fig. 3b). The seismic vault is revised including three concrete piers of 1 m width, one at the northern wall with a height of 70 cm and a length of 5 m and two at the southern wall with a height

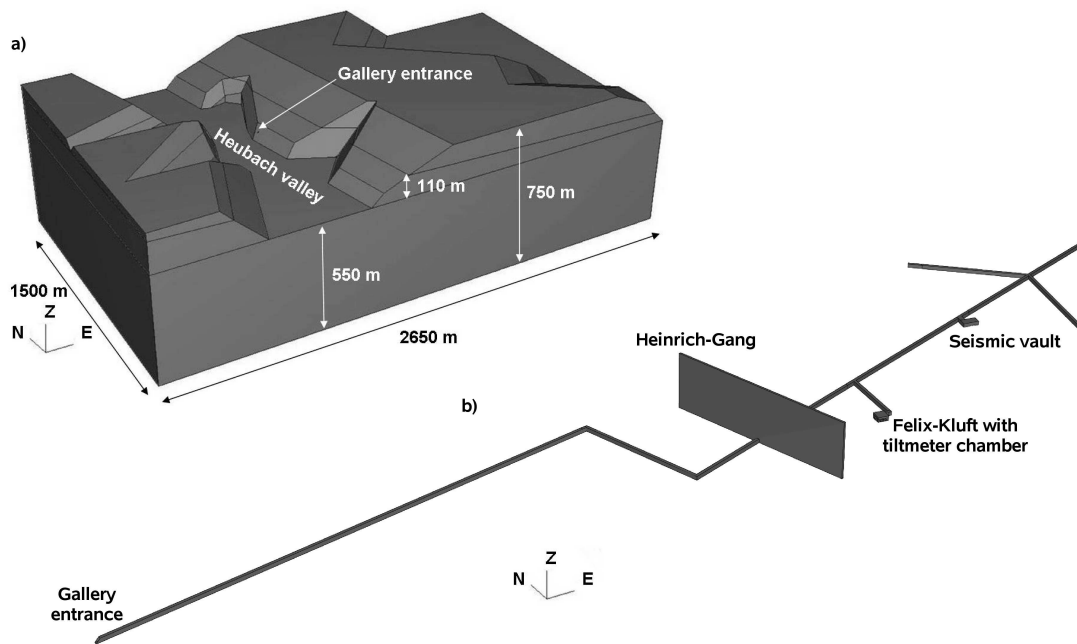


Figure 2: a) Perspective view of the BFO FE model “litho” (Steffen et al., 2006) from the southwest. b) Perspective view of the modelled gallery from the southwest.

of 25 cm and a length of 1.44 m, respectively (Fig. 3a). Between the southern piers a gap of 5 cm exists, allowing to study the tidal effects (Zürn et al., 1991).

The model is meshed with 165 000 elements (hexa- and tetrahedra), resulting in interior resolution of 0.12 cm side length in the gallery and the included cavities, and outside resolution at the top of 100 m. The model is parameterised with properties of granite and sandstone (for values see Steffen et al., 2006) for which a linear, elastic rheology is used. The gallery interior as well as the cavities are parameterised as air.

Three principle load cases are studied:

1. a uniform barometric pressure load on the model surface (valleys and mountains),
2. dynamic pressure acting on the eastern hill flank simulating wind-induced effects, and
3. the passage of pressure fronts.

Since an elastic rheology is used, the effects can be scaled and superimposed. From the loading scenarios, resulting tilts are calculated directly from nodes closest to the locations of the instruments. Special nodes were set directly at the required positions.

3 Results

Figures 4 and 5 summarise the results for the tilt induced from different load cases at 12 different locations. Four points are selected in the middle of the northern pier in the seismic vault, reflecting reasonable instrument positions. The distance in between is 1 m. They are numbered in ascending order from W to E, starting with P1 (Fig. 3a). On the southern piers also four points are chosen, two on each pier in the center with a distance in between of 48 cm. As for the northern wall, they are numbered from W to E but starting with P5. In the tiltmeter chamber two points (P9 and P10, P9 north of P10) are taken for the tilt calculation in the western niche (Fig. 3b). In the southern niches one point is selected within each niche. P11 is in the southwestern niche, P12 in the southeastern.

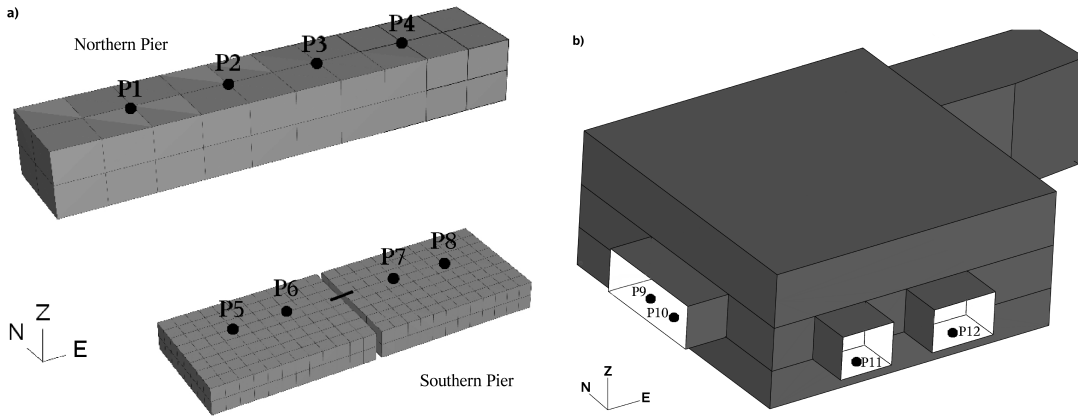


Figure 3: a) Perspective view of the piers in the seismic vaults from the southwest. b) Perspective view of the tiltmeter chamber with its niches from the southwest.

3.1 Uniform pressure and wind

Northern pier. On the northern pier for point P1 the uniform pressure load induces a tilt to E of more than 2 nrad/hPa and a tilt to N of about 1 nrad/hPa. For the other points on this pier the effect in the EW-component is reduced by a factor of up to 37 and reverse directed. In contrast to this, the NS-component only shows slight differences (around 7%) between all four points. The wind-induced effect in the EW-directions is directed westwards, where the source of pressure can be found. Surprisingly, a behaviour as for the uniform-pressure load cannot be found. In this case, the effect is around -0.2 nrad/hPa. Compared to the results of the uniform pressure, for the NS-component a reduction by a factor of 50 can be determined and the direction has changed. Thus, compared to the uniform pressure-load effect the influence of wind on the northern pier is negligible.

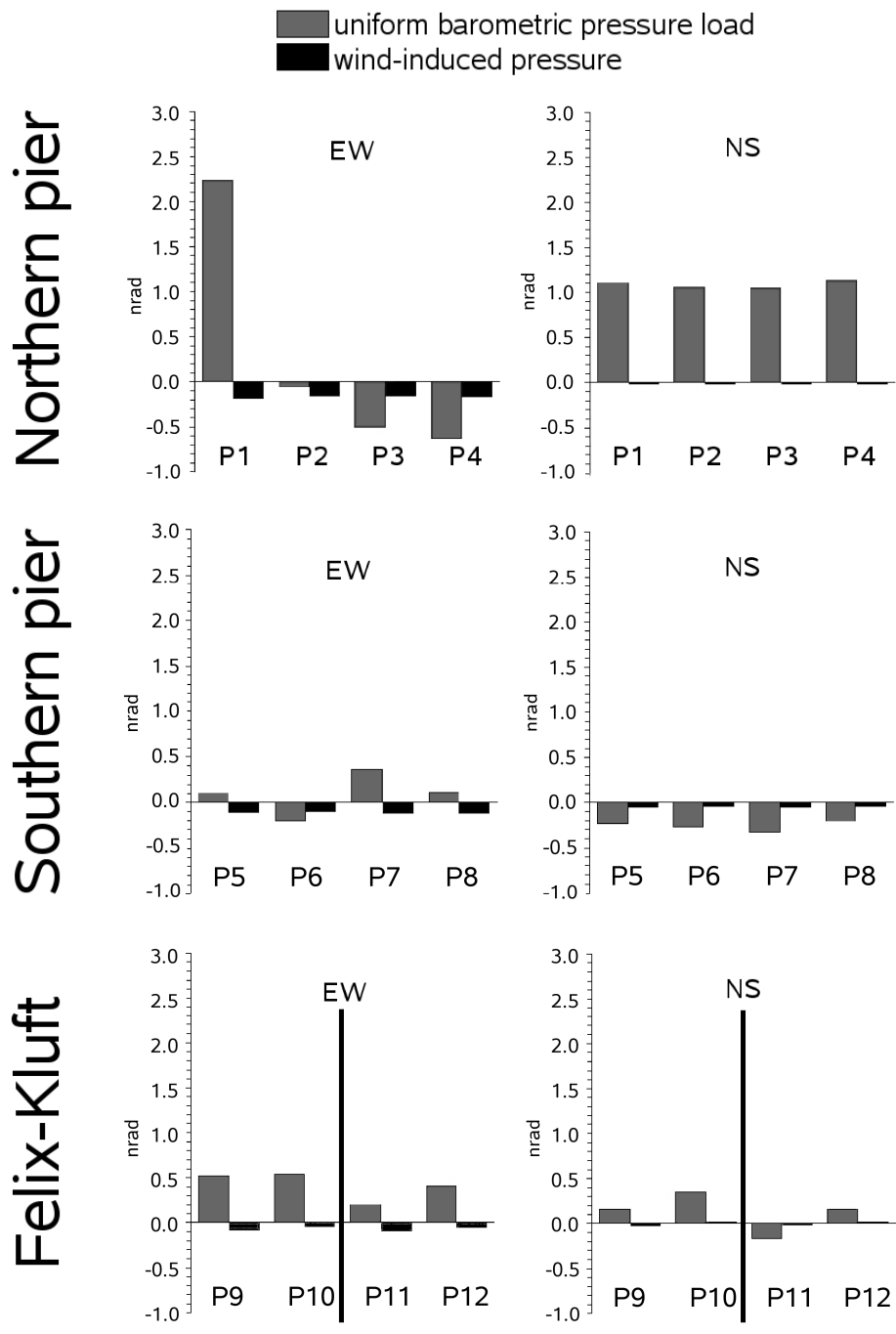


Figure 4: Tilts obtained for uniform and wind-induced pressure load normalised to 1 hPa for different locations. Top: northern pier in the seismic vault. Middle: southern piers in the seismic vault. Bottom: Niches in the Felix-Kluft. Tilt eastward, northward positive.

Southern piers. In general, the averaged tilt effects on the southern piers are smaller than the tilt effects on the northern pier, e. g. for the EW–component and the wind case, the tilt is decreased by a third. However, a comparison has to be done carefully as there are two smaller piers on the southern wall. In the uniform pressure-load case, the effects in the EW–component at P5 and P6 are reverse directed within a distance of 48 cm. For P7 and P8 a tilt eastward yields with a 3 times larger effect for P7. In contrast to the uniform pressure load, the wind affects each point with a tilt westwards of around 0.1 nrad/hPa. In the NS–component uniform pressure and wind load lead to tilts to S with nearly identically values of around 0.25 nrad/hPa and 0.05 nrad/hPa, respectively. The largest difference can be found between P7 and P8 with around 0.1 nrad/hPa.

Niches in the Felix-Kluft. The tilt for a uniform pressure load in the western niche (P9 and P10) of the tiltmeter chamber yields in a direction to E and N, while the wind induces tilts to W for both points, S for P9 and N for P10. The values are comparable with the ones from the southern pier in the seismic vault. The tilt calculated for the southern niches shows for the uniform pressure load a tilt to E in both niches. For the NS–component reverse tilts are resolved. The wind–induced effects are smaller and for the EW–component directed to W. The NS–component shows the same direction as for the uniform pressure load.

Generally, the wind-induced effects are directed to W, where the pressure is applied and are smaller than effects induced by uniform pressure. In the NS–component a tilt to S with values around and much less than 0.1 nrad/hPa is found, except for two points in the Felix-Kluft, but this might be due to local cavity effects in the niches.

3.2 Passing pressure fronts

Fig. 5 shows the tilt effects at different locations for a passing pressure front from W to E. Significant effects in both components can be found, strongly dependent on the direction of the pressure front. In the EW–component, directed in moving direction of the front, one can clearly see two peaks at all locations. The first peak is obtained when the front reaches the gallery area and is directed to W, to the source of pressure. The second peak is directed to E and confirms the tilting to the source of pressure, as in this case the end of the pressure front is above the gallery area. The tilt amplitudes of the first and second peak are different, which is caused by the topography of the mountain. This confirms earlier findings of Kroner et al. (2005) for Moxa. In the NS–component for the seismic vault a perfect example for the cavity effect can be seen (Fig. 6). On the northern pier a tilt northwards for all points and on the southern pier a tilt southwards for all points can be established. The load on the top decreases the vertical distance, which in turn leads to an increase of the NS–distance. As the piers are connected to the walls, they dip into the direction where the wall is located. In the tiltmeter chamber of the Felix-Kluft this behaviour is not observed, which is due to the more complicated structure of the chamber with three niches. In addition, the chamber is closer to the large Heinrich-Gang, which strongly influences the tilt (Steffen et al., 2006).

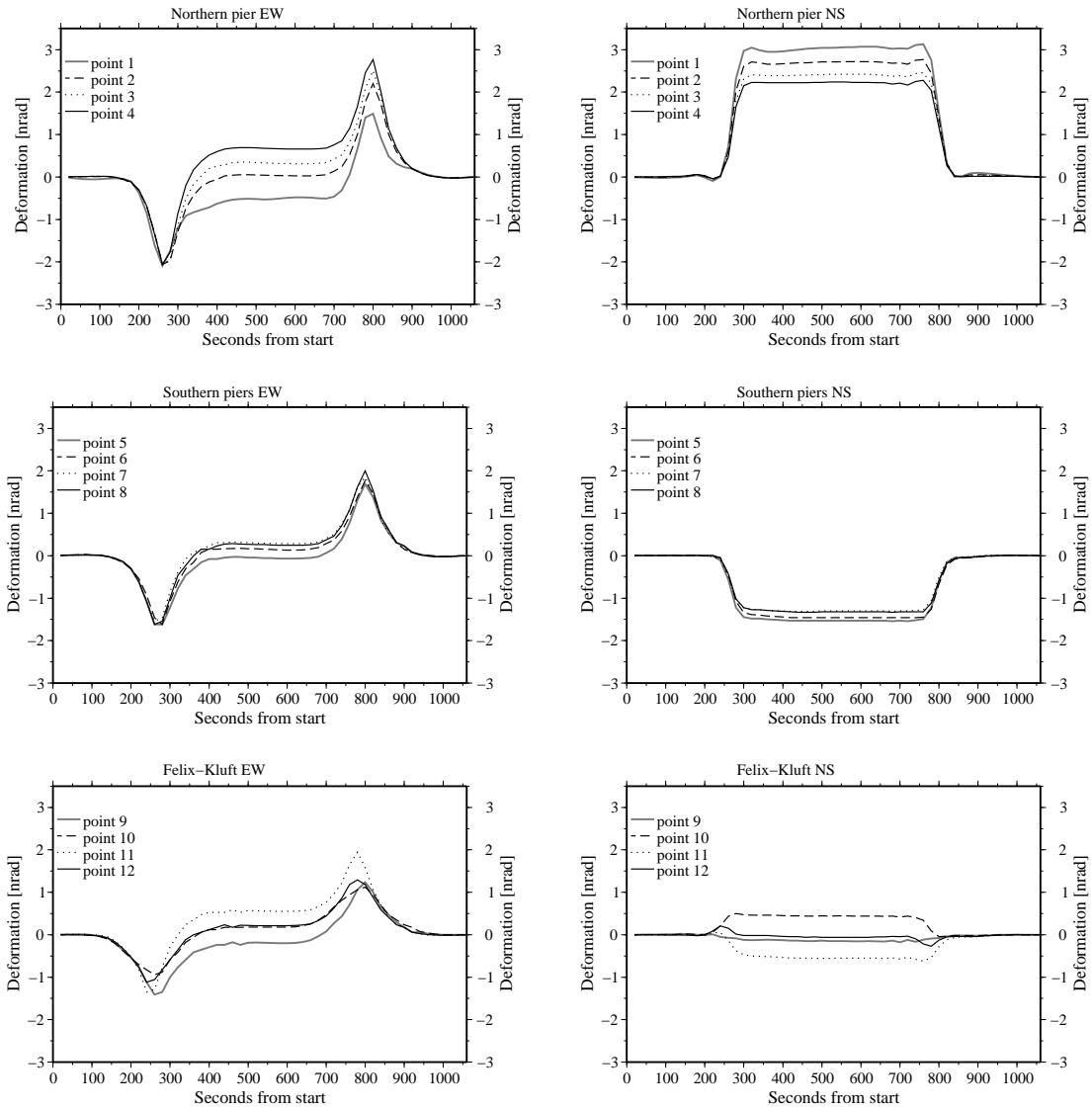


Figure 5: Tilts obtained for the traverse in time of a pressure area normalised to 1 hPa for different locations. The front is moving over the model having a velocity of 5 m/s and the model length of 2650 m. The model is loaded until the uniform pressure case is reached and afterwards unloaded. Thus, the pressure front has to cover a distance of 5300 m in 1060 s. Top: northern pier in the seismic vault. Middle: southern piers in the seismic vault. Bottom: Niches in Felix-Kluft. Tilt eastward, northward positive.

Northern pier. In the EW-component two interesting results can be found. First, the amplitudes for the first peak (tilt to W) for all points are nearly the same, while for the second peak (tilt to E) differences of more than 1 nrad/hPa result. Second, the smallest effects can be obtained for P2 and P3 when the gallery area is loaded as for the uniform pressure load. In the NS-component the difference of 1 nrad/hPa yields

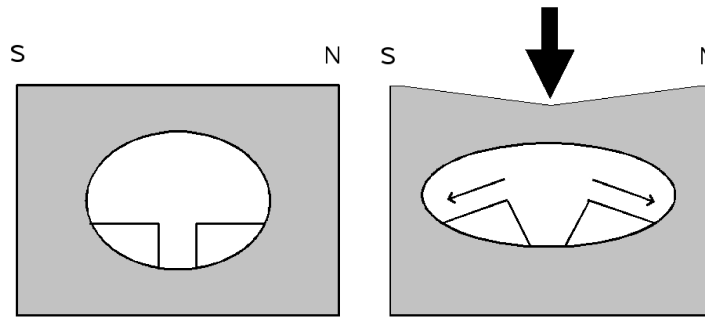


Figure 6: Sketch of the cavity effect in the seismic vault.

again, but all points are influenced by a constant value over a large load period. The difference in the amplitude between the peaks is a result of the topography, while the difference between the tilt of the points is due to the location on the pier.

Southern piers. In both components all points show nearly the same tilting. Compared to the northern pier, the amplitudes in both components are smaller with up to 1 nrad/hPa. In the EW-component, the amplitudes of the first peak are smaller by around 0.5 nrad/hPa than the amplitudes of the second peak, which is as mentioned before due to the topography. In the case of a pressure front, the instrument's position on the southern piers seems to be negligible. This might be due to the smaller height compared to the northern pier and/or the gap between the piers.

Niches in the Felix-Kluft. At first, the effects in western niche will be discussed. The EW-component for both points shows the already discussed tilting over time dependent on the pressure front. Interestingly, P9 is more affected with larger tilts in the first peak and in the time of continuous load over the gallery. In the NS-component P9 is slightly influenced, while P10 is more affected with a tilt northwards. The largest effects in the EW-component of all points in the tiltmeter chamber can be found for P11 in the southwestern niche. Point P12 in the southeastern niche shows effects like P10. A tilt southwards can be observed for P11 in the NS-component. In contrast to this, only small tilts with eye-catching peaks can be established for P12. They behave like the EW-component reverse directed arising from the geometry of the chamber and the niches.

4 Conclusions

A FE model was used in this work to understand barometric pressure-induced signals in horizontal seismometer and tiltmeter records. Here, the influence of an uniform pressure load, the effect of wind-induced pressure and the influence by a passage of a pressure front were investigated and compared for different instrument sites at the BFO. Significant tilts affecting the records can be found for all load cases. We have shown that the location of an instrument is of importance. Resulting effects at the

BFO can differ in the direction and the amplitude within less than 50 cm. Furthermore, differences of up to a factor of 37 within 1 m distance are found. The biggest effects can be found on the northern pier in the seismic vault. Wind-induced pressure applied in the valley west of the observatory leads to effects with bigger magnitudes in EW-component, directed westwards to the source of the pressure, while the NS-component, which is directed perpendicular to the pressure source, shows only small effects. It is also shown that tilt effects are dependent on the direction of a passing barometric pressure event, which confirms earlier findings from Kroner et al. (2005) for Moxa.

Steffen et al. (2006) suggested three important conclusions for a correction. Regarding the results of Kroner et al. (2005), Steffen et al. (2006) and this work one contribution to point 3 has to be added. Thus, for a correction the three important conclusions are:

1. Each observatory requires a correction for barometric pressure effects adapted to its local conditions.
2. Each component requires its own correction.
3. A barometric pressure correction should take into account at least contributions by
 - a uniform, constant pressure load, and
 - wind-related pressure on the flanks of the observatory surroundings, **and**
 - **passing pressure fronts.**

Acknowledgments

The author wants to thank Walter Zürn, Corinna Kroner, Thomas Jahr, Sonja Kuhlmann and Kasper D. Fischer for many fruitful discussions. Georg Kaufmann is thanked for helpful comments on an earlier version of this paper. The FE modelling is carried out with the software ABAQUS.

References

- Beauduin, R., Lognonne, P., Montagner, J. – P., Cacho, S., Karczewski, J. F. & Morand, M. 1996. The effects of the atmospheric pressure changes on seismic signals or how to improve the quality of a station. *BSSA* **86**, pp. 1760–1769.
- Emter, D., Wenzel, H.-G. & Zürn, W. 1999. Das Observatorium Schiltach. *Mittlg. d. DGG* 3/1999: pp. 2-15.

- Fischer, K. D. 2002. Sources and transfer mechanism of seismic noise: Preliminary results from FEM models. *Bull. d'Inf. Marees Terr.* **137**, 10881–10886.
- Freybourger, M., Hinderer, J. & Trampert, J. 1997. Comparative study of superconducting gravimeters and broadband seismometers STS-1/Z in seismic and subseismic frequency bands. *Phys. Earth planet. Inter.* **101**: pp. 203-217.
- Kroner, C., Jahr, Th., Kuhlmann, S. & Fischer, K. D. 2005. Pressure-induced noise on horizontal seismometer and strainmeter records evaluated by finite element modelling. *Geophys. J. Int.* **161**: pp. 167–178, doi:10.1111/j.1365-246X.2005.02576.x.
- Lambotte, S., Rivera, L., & Hinderer, J. 2006. Vertical and horizontal seismometric observations of tides. *J. Geodyn.* **41**(1-3), pp. 39–58.
- Sorrels, G. G. 1971. A preliminary investigation into the relationship between long-period seismic noise and local fluctuations in the atmospheric pressure field. *Geophys. J. R. Astr. Soc.* **26**, pp. 71–82.
- Sorrels, G. G., McDonald, J. A., Der, Z. A. & Herrin, E. 1971. Earth motion caused by local atmospheric pressure changes. *Geophys. J. R. Astr. Soc.* **26**, pp. 83–98.
- Steffen, H., Kuhlmann, S., Jahr, Th. & Kroner, C. 2006. Numerical modelling of the barometric pressure-induced noise in horizontal components for the observatories Moxa and Schiltach. *J. Geodyn.* **41**, pp. 242–252, doi:10.1016/j.jog.2005.08.011.
- Zürn, W. 2002. Simplistic models of vertical noise above 0.1 mHz derived from local barometric pressure. *Bull. d'Inf. Mareés Terr.* **137**, pp. 10867–10874.
- Zürn, W. & Neumann, U. 2002. Simplistic models of atmospheric signals in horizontal seismograms. *Bull. d'Inf. Marees Terr.* **137**, pp. 10875–10880.
- Zürn, W. & Wielandt, E. 2006. On the minimum of vertical seismic noise near 3 mHz. *Geophys. J. Int.*, submitted.
- Zürn, W., Emter, D. & Otto, H. 1991. Ultra-short strainmeters: Tides are in the smallest cracks. *Bull. d'Inf. Mareés Terr.* **109**, pp. 7912–7921.
- Zürn, W., Exss, J., Kroner, C., Jahr, T., Steffen, H. & Westerhaus, M. 2006. On the reduction of long period horizontal seismic noise using local barometric pressure. *Geophys. J. Int.*, in prep.